EUROPEAN UNION
European Structural and Investment Funds
Operational Programme Research,
Development and Education

FZU Institute of Physics of the Czech Academy of Sciences

Optical spectroscopy and biosensors for investigation of biomolecules and their interactions

Jakub Dostalek

AIT - Austrian Institute of Technology GmbH
Biosensor Technologies Unit
Konrad-Lorenz-Strasse 24 | 3430 Tulln | Austria
T +43(0) 664 2351773

FZU – Institute of Physics of the Czech Academy of Sciences,
Na Slovance 1 | Prague 182 00 | Czech Republic
T+420 776767927

jakub.dostalek@ait.ac.at | http://www.ait.ac.at | http://www.jakubdostalek.cz

Surface Plasmon Resonance Biosensors I

Content

- Design of a flow-cell chamber in affinity biosensors.
- Principle of SPR biosensors.
- Propagating surface plasmons (PSPs) on metallic films - optical configurations for the coupling (ATR, grating).
- Localized surface plasmons on metallic nanostructures attached to solid substrates.
- Angular and wavelength interrogation of SPR
- Surface mass density measurements with SPR biosensors

Microfluidic Chamber in Affinity Biosensors

Example of a Study on the Flow-cell Geometry Impact on Affinity Binding Kinetics

Lab on a Chip

RSC Publishing

PAPER

Enhancement of affinity-based biosensors: effect of sensing chamber geometry on sensitivity

Cite this: *Lab Chip*, 2013, 13, 1413

N. Scott Lynn Jr., Hana Šípová, Pavel Adam and Jiří Homola*

https://pubs.rsc.org/en/Content/ArticleLanding/2013/LC/c2lc41184a#!divAbstract

Flow-Cell Geometry

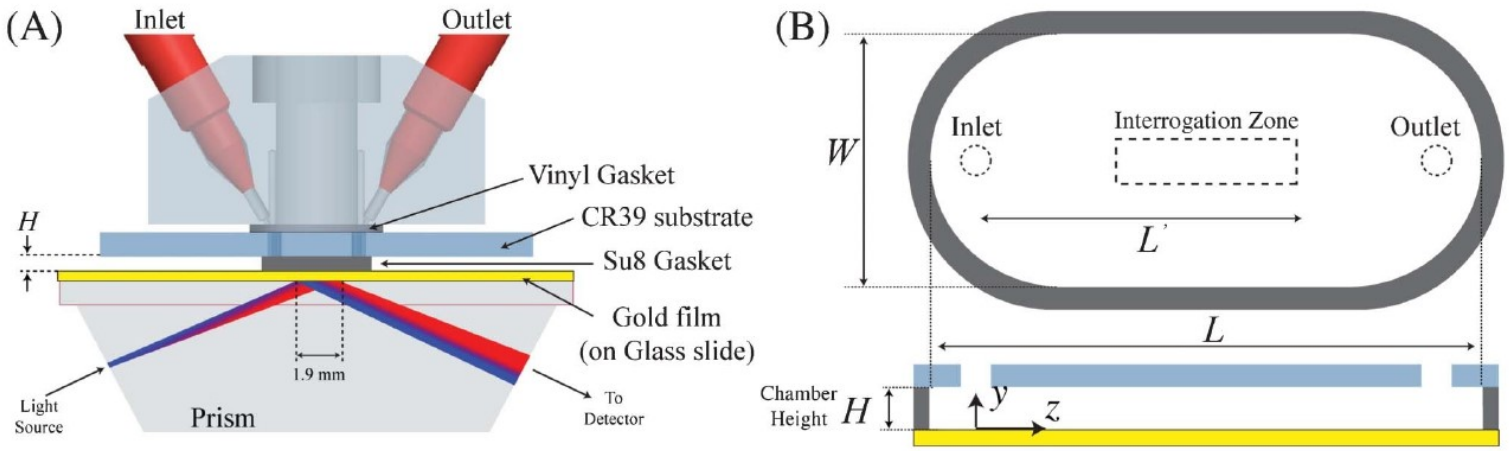

Fig. 1 (A) Detail of the SPR sensor head used in the experimental portion of this study. We utilize an SU-8 gasket to seal the sensing head to the gold surface, which acts as the sensor floor. (B) Geometry of the sensing chamber used in this study.

Table 1 List of parameters utilized in this study

Parameter	Description	Value
L	Length of flow cell	6 mm
H	Height of flow cell	5–50 μm
W	Width of flow cell	2.8 mm
Q	Volumetric flow rate	0.5 $mm^3\ s^{-1}$
D	Analyte diffusivity	$10^{-4}\ mm^2\ s^{-1}$
$C_{B,o}$	Surface density of probes	$4 \times 10^{-14}\ mol\ mm^{-2}$
k_1	Forward reaction coefficient	$10^7\ M^{-1}\ s^{-1}$
k_2	Reverse reaction coefficient	$6 \times 10^{-5}\ s^{-1}$

- Example of a typical flow cell geometry with a zone where optical readout is performed.

Flow-rate Dependence of a Flux of Biomolecules to the Surface

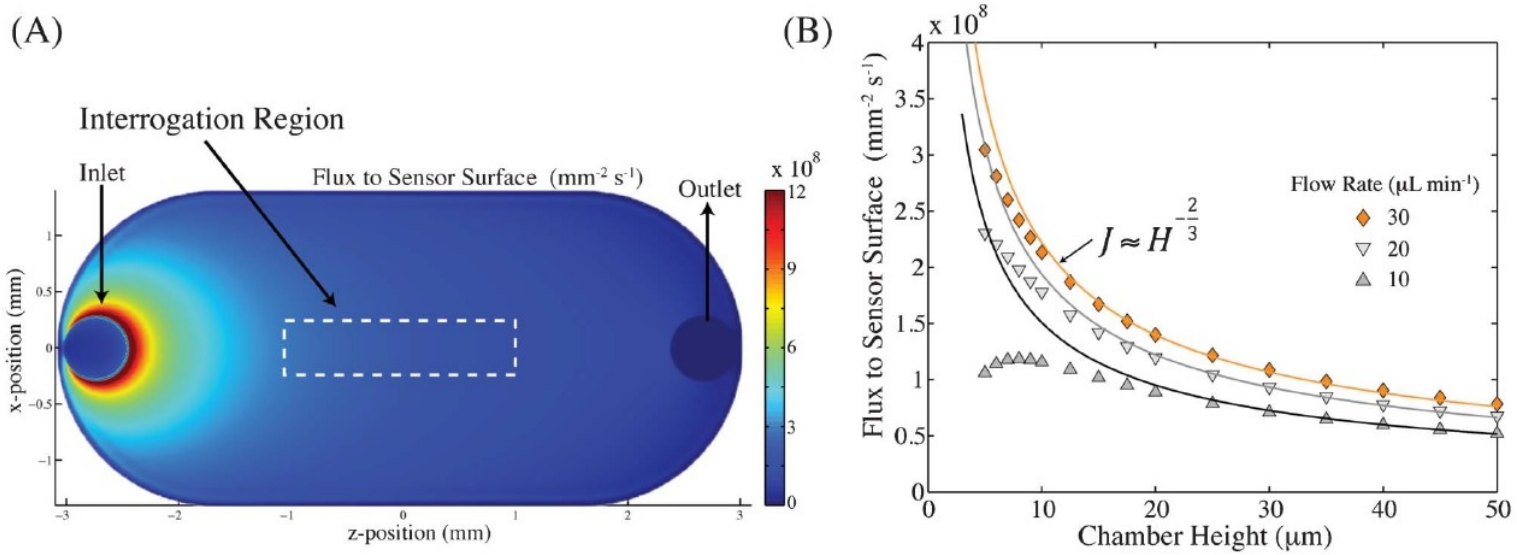

Fig. 3 (A) COMSOL results regarding the flux of an analyte (J) to the sensor chamber floor for a sensor with H = 5 μm, Q = 30 μL min^{-1}, and $C_{A,o}$ = 20 nM. The interrogation region is shown as the white box and is positioned in the center of the chamber. (B) The analyte flux averaged over the interrogation region as a function of the chamber height H. The data points for H > 15 μm were fit to the equation $J = aH^{-\frac{2}{3}}$, plotted as the solid lines.

- The binding events are depending on the location with the flow chamber and depends on the geometry parameters.

Height Dependence of a Flux of Biomolecules to the Surface

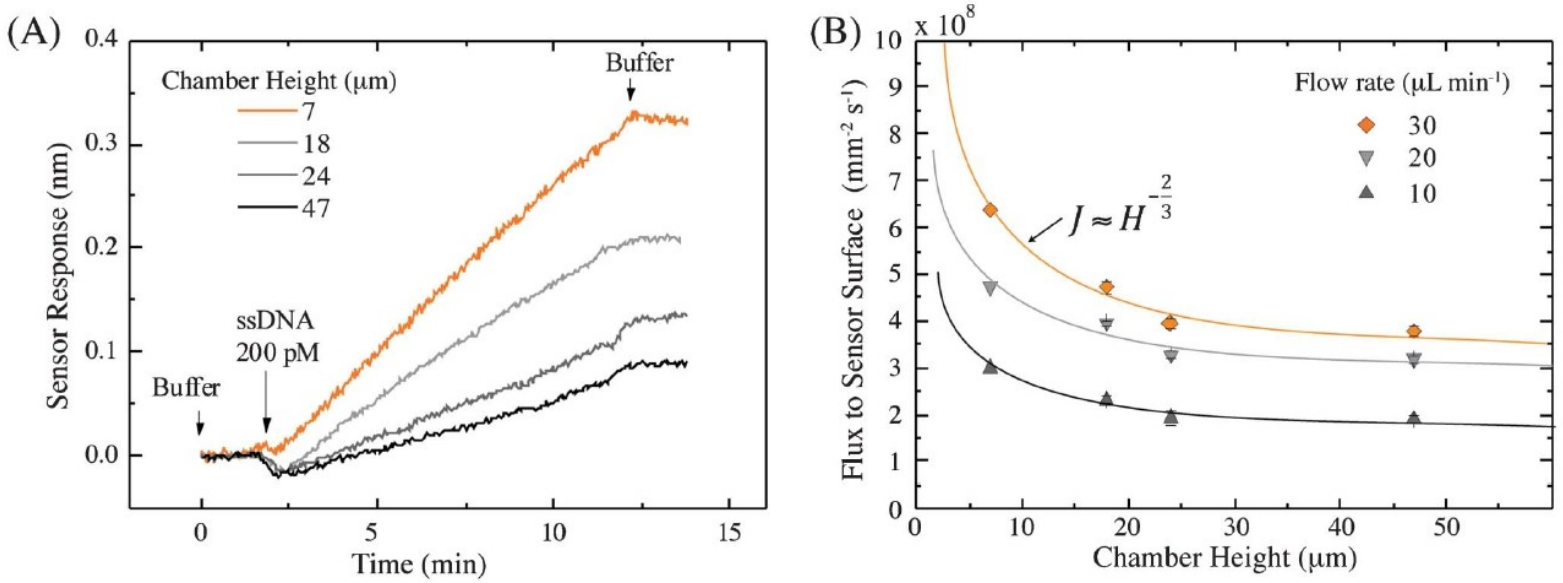

Fig. 4 (A) Sensor response *vs.* time for the direct detection of 200 pM ssDNA. (B) Calculated ssDNA flux to the sensor as a function of chamber height ($C_{A,o}$ = 20 nM). The solid lines represent a fit of the data to a $H^{-\frac{2}{3}}$ scaling law.

- The binding events are depending on the location with the flow chamber and depends on the geometry parameters.

Diffusion-Limited Binding Kinetics

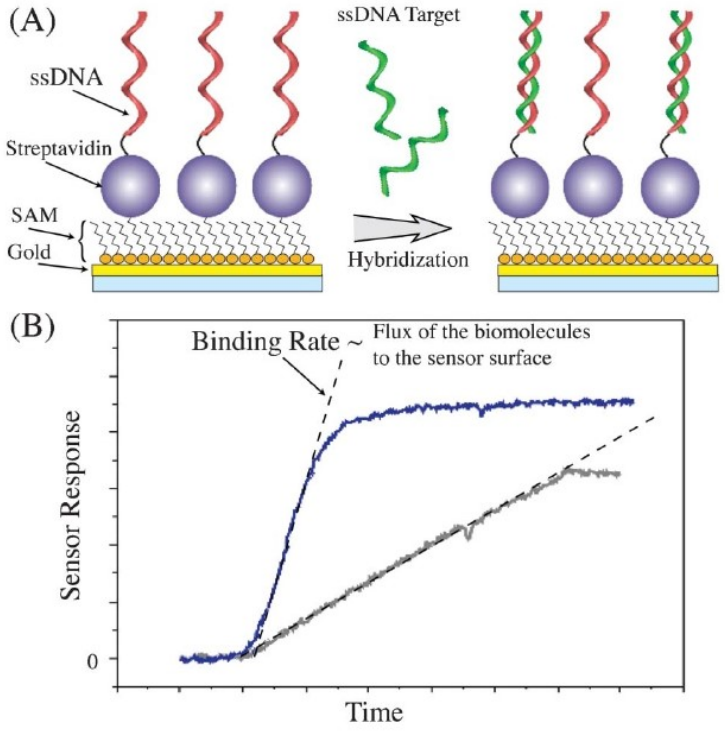

Fig. 2 (A) Scheme of a model biomolecular interaction used in this study. Biotinylated ssDNA is immobilized to a streptavidin layer that is bound to a self-assembled monolayer (SAM) of alkanethiols present on the sensor surface. (B) The typical sensor response *vs.* time, where the blue and grey data sets were taken with higher and lower concentrations of target ssDNA, respectively. The slope of the time-series response is proportional to the flux of analyte to the sensor surface.

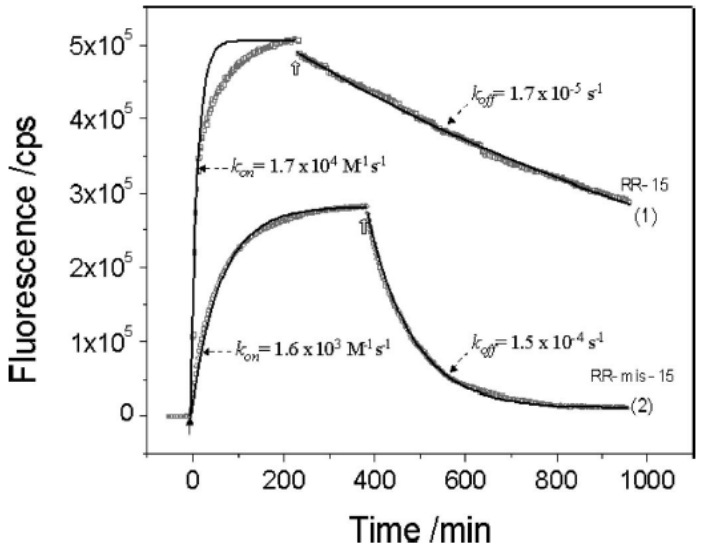

H. Park, A. Germini, S. Sforza, R. Corradini, R. Marchelli, and Knoll W. ,BioInterphases **1, 113 2006.**

Principle of SPR Biosensors

EUROPEAN UNION
European Structural and Investment Funds
Operational Programme Research, Development and Education

MINISTRY OF EDUCATION, YOUTH AND SPORTS

FZU Institute of Physics of the Czech Academy of Sciences

AIT AUSTRIAN INSTITUTE OF TECHNOLOGY

Probing of Affinity Binding Events

The capture of target analyte on the sensor surface forms an additional layer with increased refractive index δn_d which is probed by surface plasmon resonance:

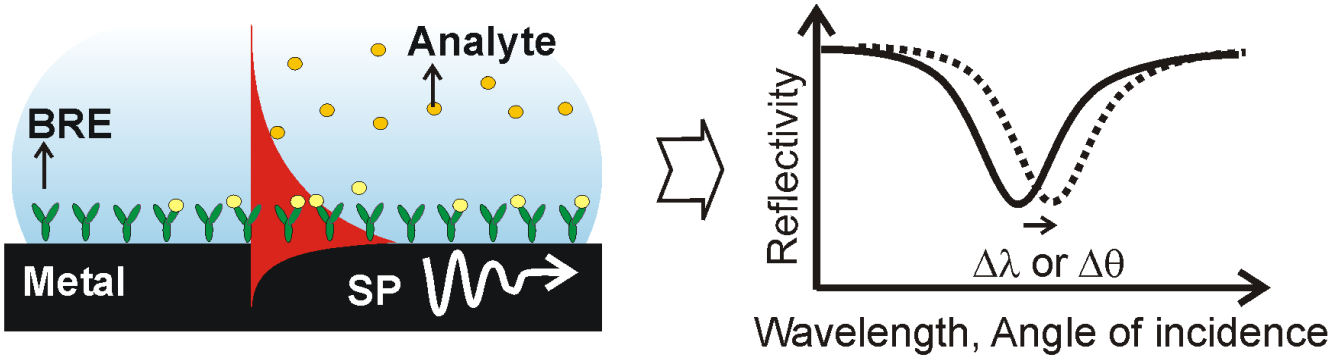

Analyte binding ⇒ Refractive index change δn_d ⇒ SP propagation constant change $\delta\beta$ ⇒ Coupling condition change $\delta\lambda$ or $\delta\theta$

Metallic Waveguides – Propagating Surface Plasmons (PSP)

Surface plasmons (SPs) or also called surface plasmon polaritons (SPPs) are waves originating from coupled oscillations of electron plasma density and associated electromagnetic field on a metal – dielectric interface.

They travel along single interface which serves a waveguide.

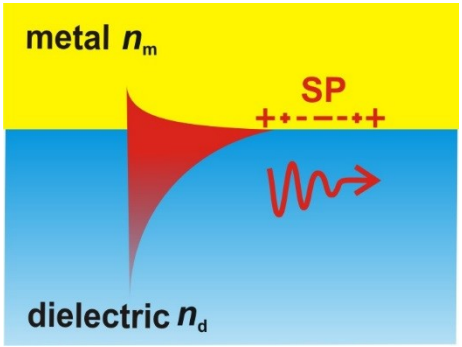

Propagation constant β can be analytically expressed as:

$$\beta = \frac{2\pi}{\lambda}\sqrt{\frac{n_m^2 n_d^2}{n_m^2 + n_d^2}}$$

- SPs allows for tight confinement of electromagnetic field at the interface.
- For visible near infrared wavelength typically gold and silver is used where the $\mathrm{Re}\{n_m^2\}<0$.
- Majority of the field is probing the dielectric n_d.

EUROPEAN UNION
European Structural and Investment Funds
Operational Programme Research, Development and Education

MINISTRY OF EDUCATION, YOUTH AND SPORTS

FZU Institute of Physics of the Czech Academy of Sciences

AIT AUSTRIAN INSTITUTE OF TECHNOLOGY

Coupling to PSPs

Grating coupling

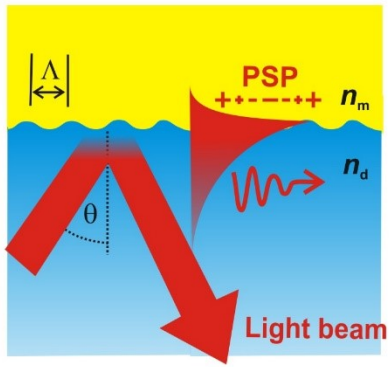

(a)

Prism coupling

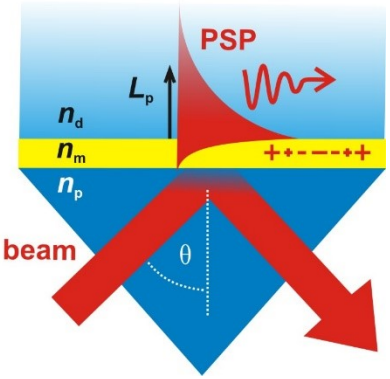

(b)

Phase-matching condition:

$$\beta = \frac{2\pi}{\lambda}\sqrt{\frac{n_m^2 n_d^2}{n_m^2 + n_d^2}}$$

a) $$\mathrm{Re}\{\beta\} = \frac{2\pi}{\lambda} n_d \sin(\theta) \pm p\frac{2\pi}{\Lambda}$$

b) $$\mathrm{Re}\{\beta\} = \frac{2\pi}{\lambda} n_p \sin(\theta)$$

- Resonant effect, coupling occurs only for certain combinations of λ and θ, where the phase-matching is fulfilled.

Grating Coupling to PSPs

$$\mathrm{Re}\{\beta\} = \frac{2\pi}{\lambda} n_d \sin(\theta) \pm p\frac{2\pi}{\Lambda}$$

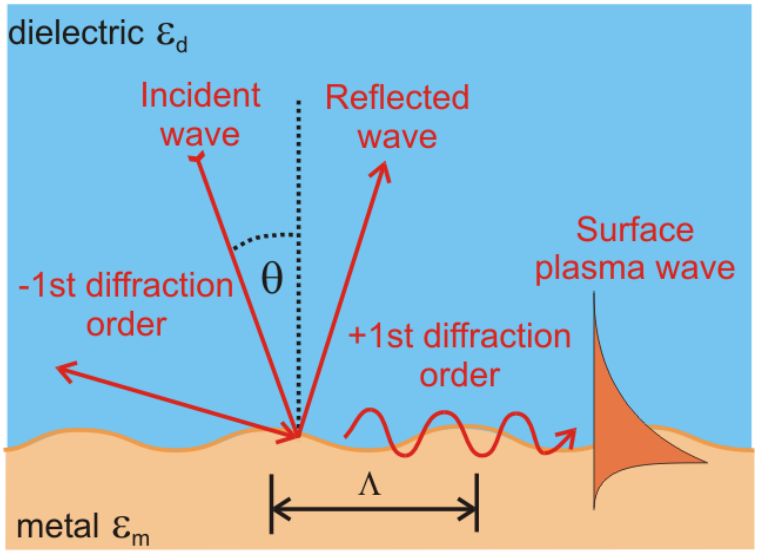

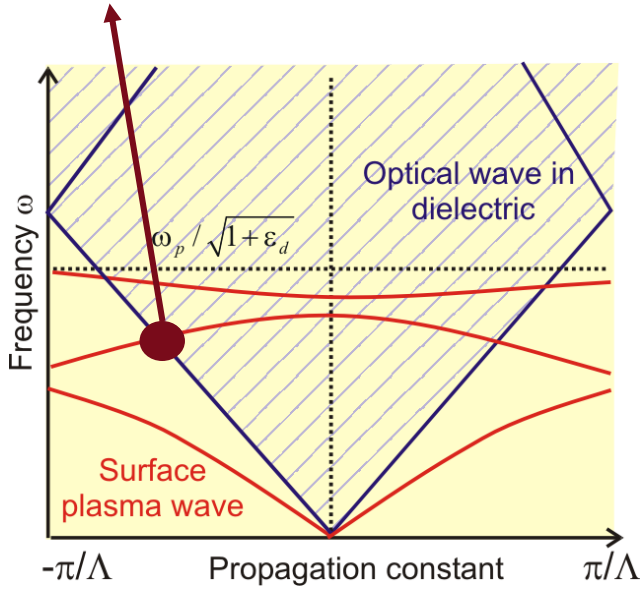

- Phase-matching can be investigated by using dispersion of the modes, manifested as a cross-section for certain diffraction order *p*.

EUROPEAN UNION
European Structural and Investment Funds
Operational Programme Research,
Development and Education

MINISTRY OF EDUCATION, YOUTH AND SPORTS

FZU Institute of Physics of the Czech Academy of Sciences

AIT AUSTRIAN INSTITUTE OF TECHNOLOGY

Grating Coupling to PSPs

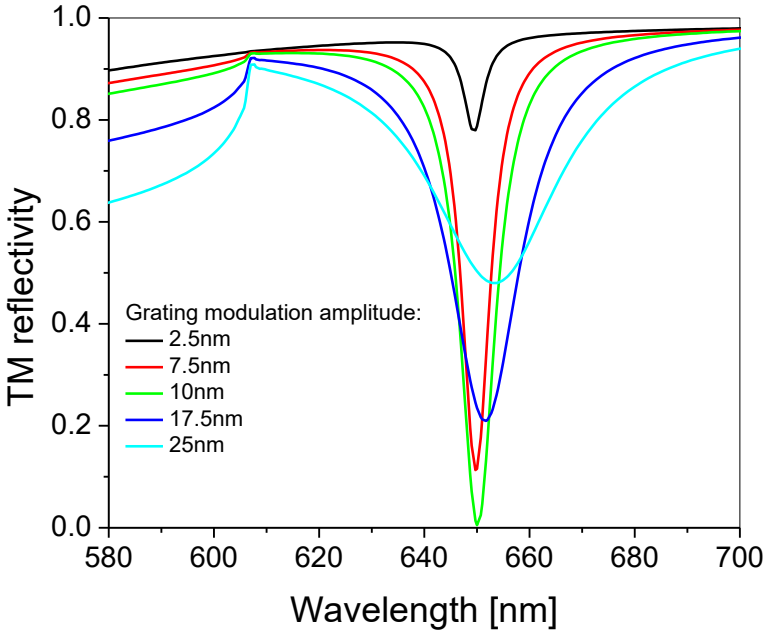

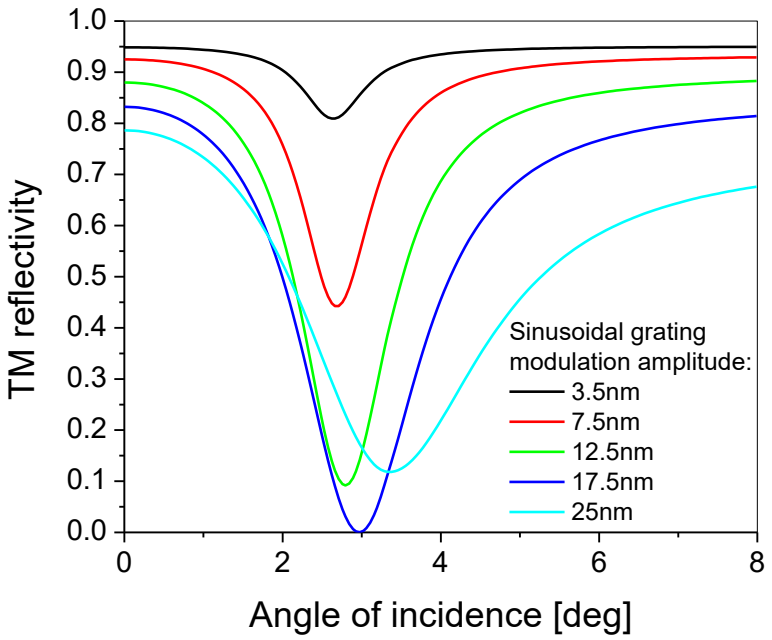

- On metallic diffraction gratings, the coupling strength to PSPs is controlled by the modulation depth.

Prism Coupling to PSPs

$$\mathrm{Re}\{\beta\} = \frac{2\pi}{\lambda} n_p \sin(\theta)$$

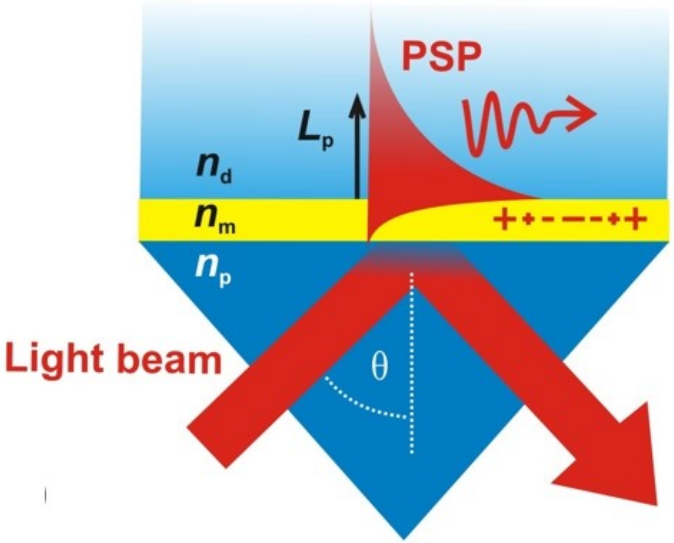

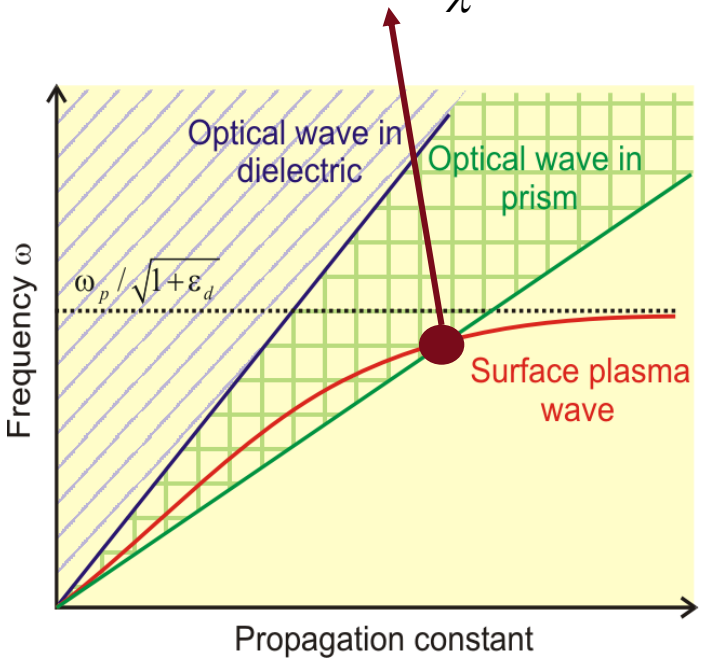

- Phase-matching by using prism is enabled by increasing the momentum of incident optical wave by using high refractive index glass n_p.

Propagating Surface Plasmons (PSP)

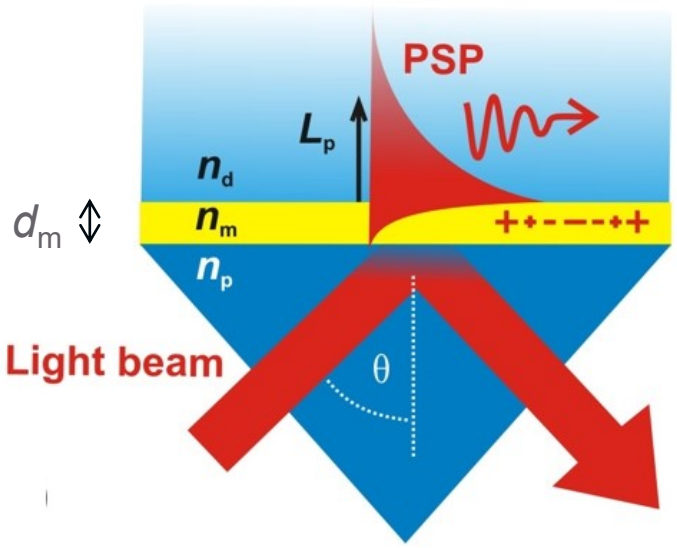

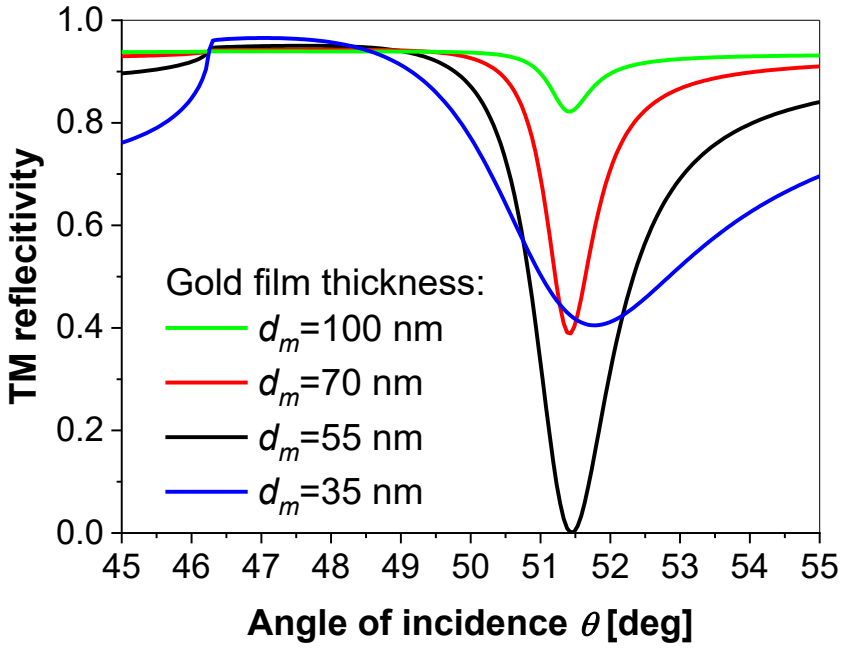

- For the ATR prism-based excitation of PSPs, the strength of the coupling is controlled by the thickness of the metal layer d_m.

EUROPEAN UNION
European Structural and Investment Funds
Operational Programme Research, Development and Education

MINISTRY OF EDUCATION, YOUTH AND SPORTS

FZU Institute of Physics of the Czech Academy of Sciences

AIT AUSTRIAN INSTITUTE OF TECHNOLOGY

'Mainz' Design of SPR Biosensor

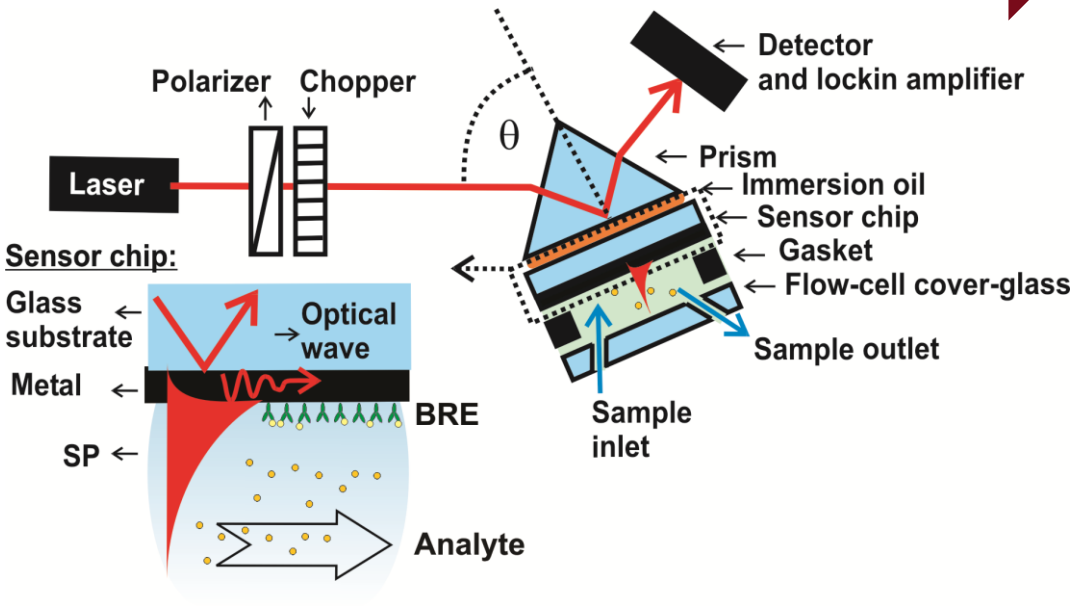

SPR reflectivity

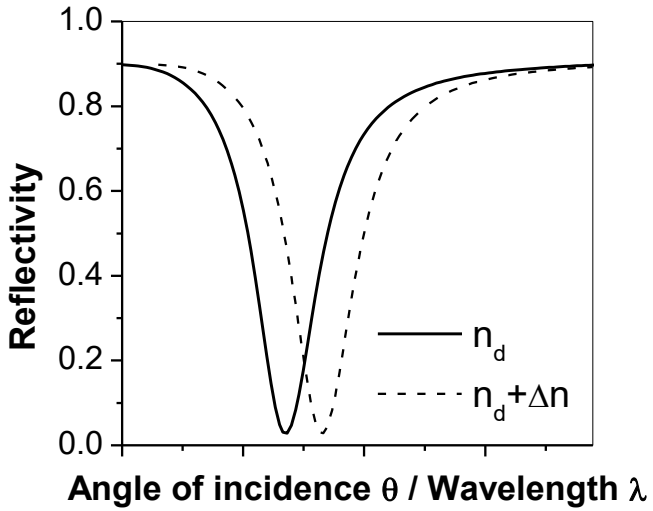

Tracking of SPR angle

Example of an optical setup of angular modulation of SPR with a micro-fluidic unit for monitoring of affinity binding

Analysis of reaction kinetics

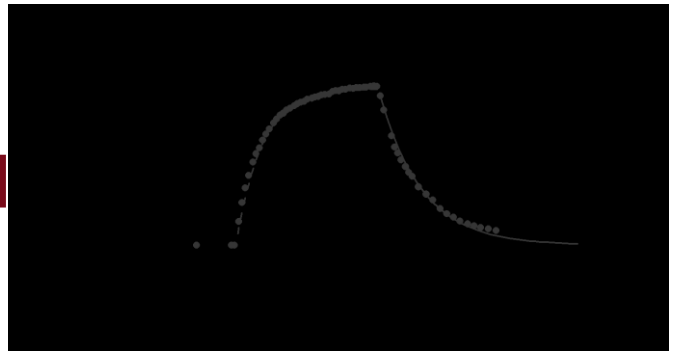

Refractive Index Sensitivity – Angular Interrogation

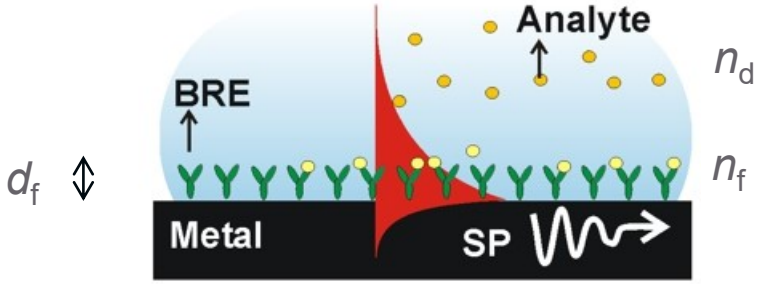

- SPR changes with both changes in the bulk n_d and surface refractive index changes.

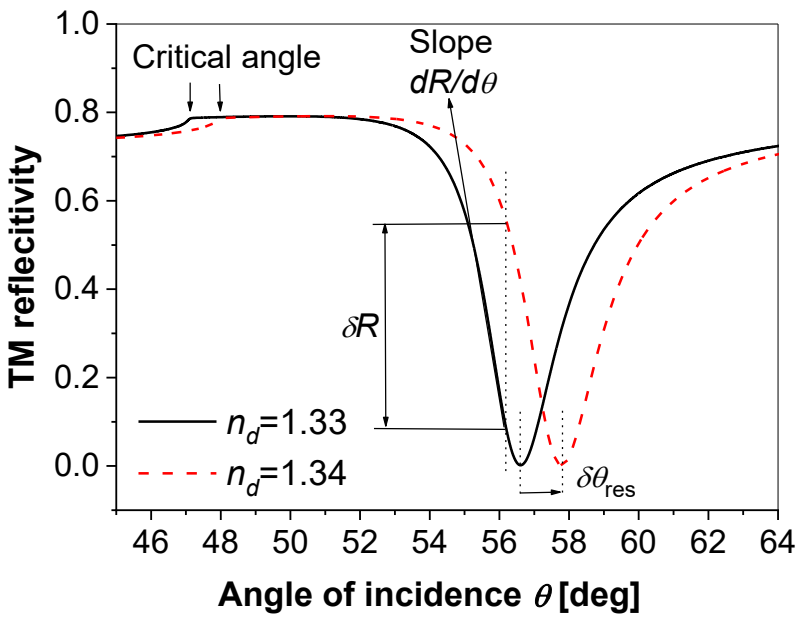

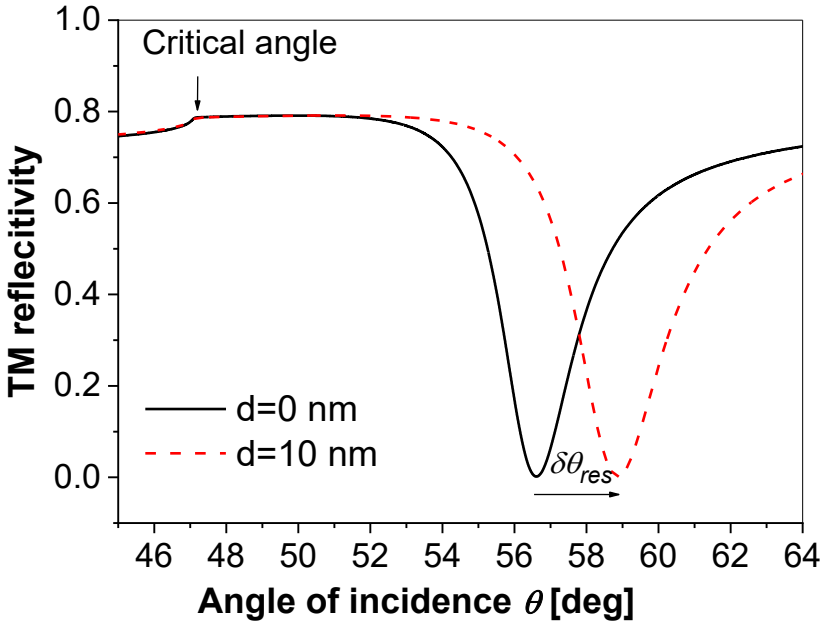

'Mainz' Design of SPR – Typical Characteristics

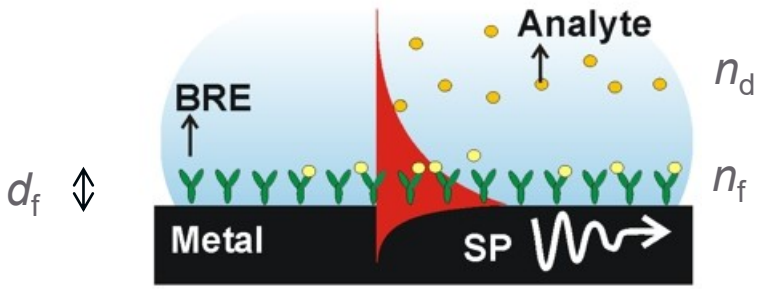

$$\delta\theta_{res} = \delta R / \left(dR / d\theta \right)$$

Bulk sensitivity:

$$\delta\theta_{res} = S_b \delta n_d$$

Surface sensitivity:

$$\delta\theta_{res} = S_s \delta n_f d$$

Surface mass density change:

$$\gamma = \frac{\delta\theta_{res}}{S} \frac{\partial c}{\partial n_f}$$

SPR prism coupler		Sensitivity of RI changes and molecular binding	
Prism refractive index	n_p=1.845	Bulk RI sensitivity	S_b=118 deg
Gold film thickness	d_m=55 nm	Surface RI sensitivity	S_s=1.28 deg nm^{-1}
Gold film refractive index	n_m=0.1+3.5i	Protein induced RI	$\partial c/\partial n_f$=0.14-0.2 µL mg^{-1}
Sample refractive index	n_d=1.33	Surface conc. ($d<<L^d_{pen}$)	γ=3-5 $\delta\theta_{res}$ ng mm^{-2}deg^{-1}

Localized Surface Plasmons (LSPs)

Localized surface plasmons (LSPs) are associated with electron plasma density oscillations on metallic nanoparticles. Provides unique optical / plasmonic characteristics.

Resonant effect, e.g. for spherical metallic nanoparticle with $d<<\lambda$ the resonance wavelength λ_{LSPR} obeys:

$$\mathrm{Re}\{n_m^2(\lambda)\} + 2n_d(\lambda) = 0$$

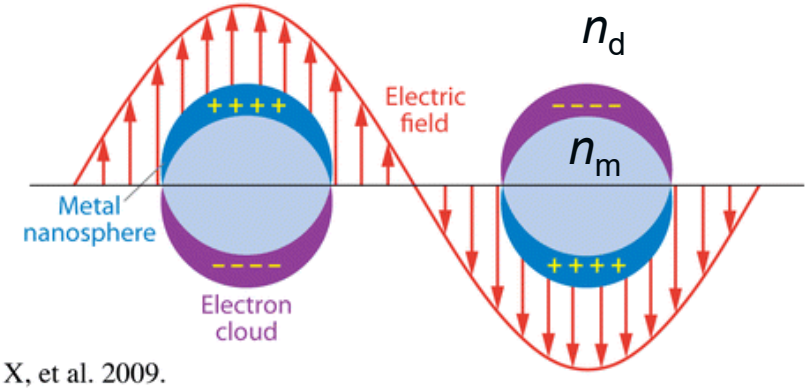

Lu X, et al. 2009.
Annu. Rev. Phys. Chem. 60:167–92

Localized surface plasmon resonance is associated with strong:

- **Absorption**
- **Scattering**
- **Field confinement and enhancement**

Localized Surface Plasmon Resonance (LSPs)

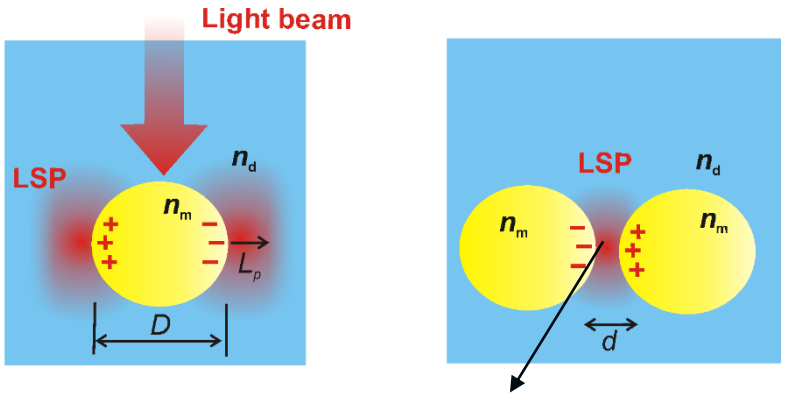

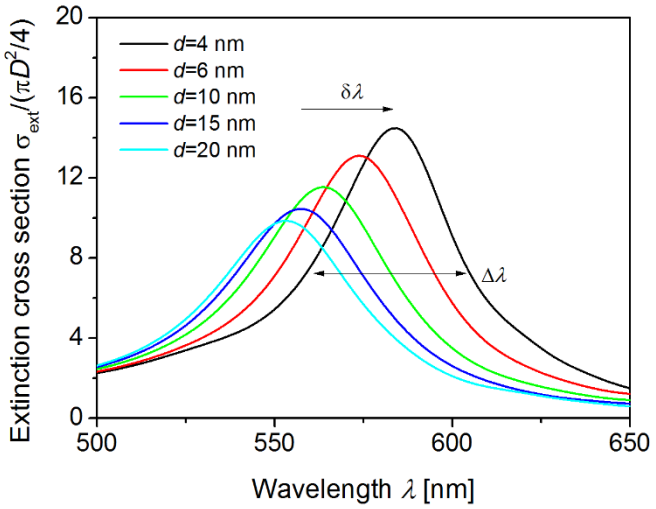

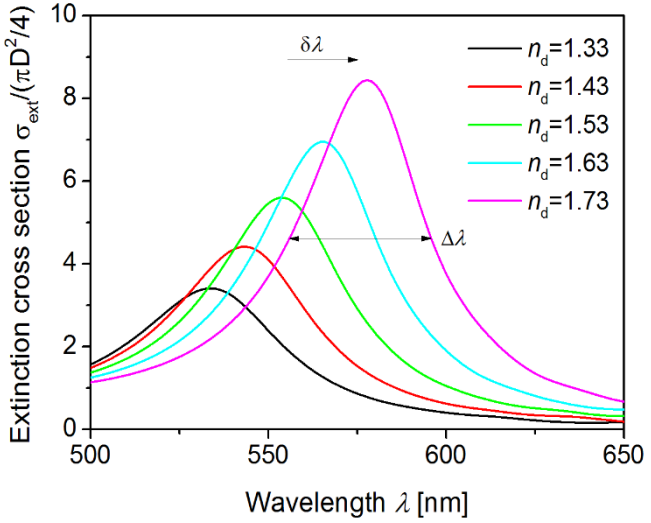

- Resonant effect, e.g. for spherical metallic nanoparticle with $D<<\lambda$ the resonance wavelength λ_{LSPR}.
- Confined electromagnetic field intensity, $L_p \sim D$.

Implementations of LSPR Biosensor

LSPR transmission

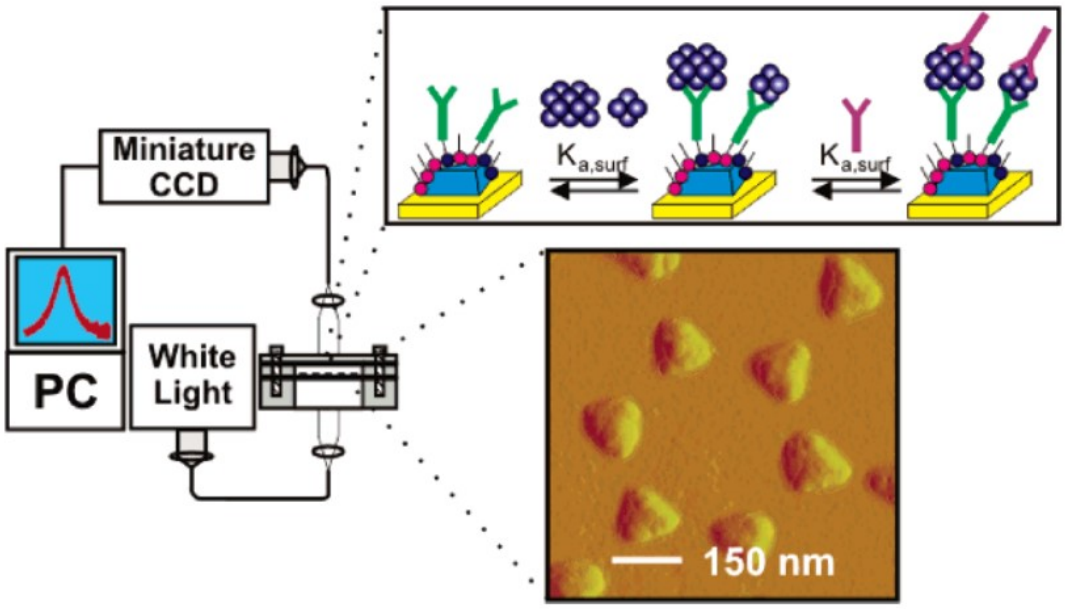

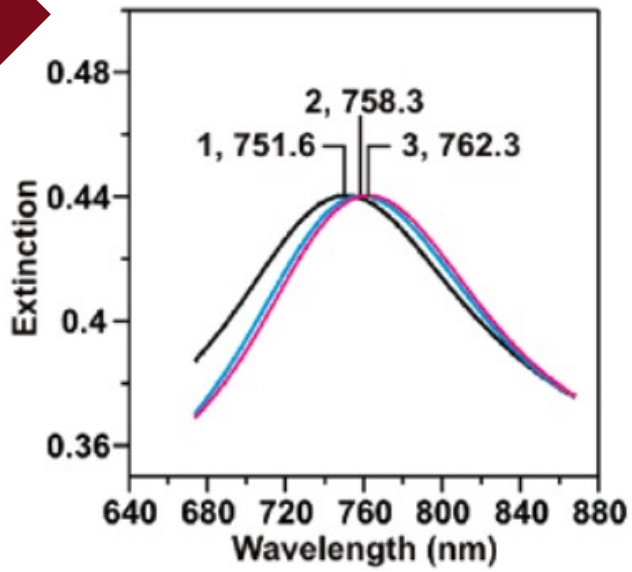

Example of first implementation of LSPR for analysis of biomarkers.

Tracking of LSPR wavelength λ_{LSPR}

A.J. Haes et al,, *J. Am. Chem. Soc.*, **2005**, *127* (7), pp 2264–2271
DOI: 10.1021/ja044087q

EUROPEAN UNION
European Structural and Investment Funds
Operational Programme Research, Development and Education
MINISTRY OF EDUCATION, YOUTH AND SPORTS
FZU Institute of Physics of the Czech Academy of Sciences
AIT AUSTRIAN INSTITUTE OF TECHNOLOGY

Refractive Index Sensitivity – Wavelength Interrogation

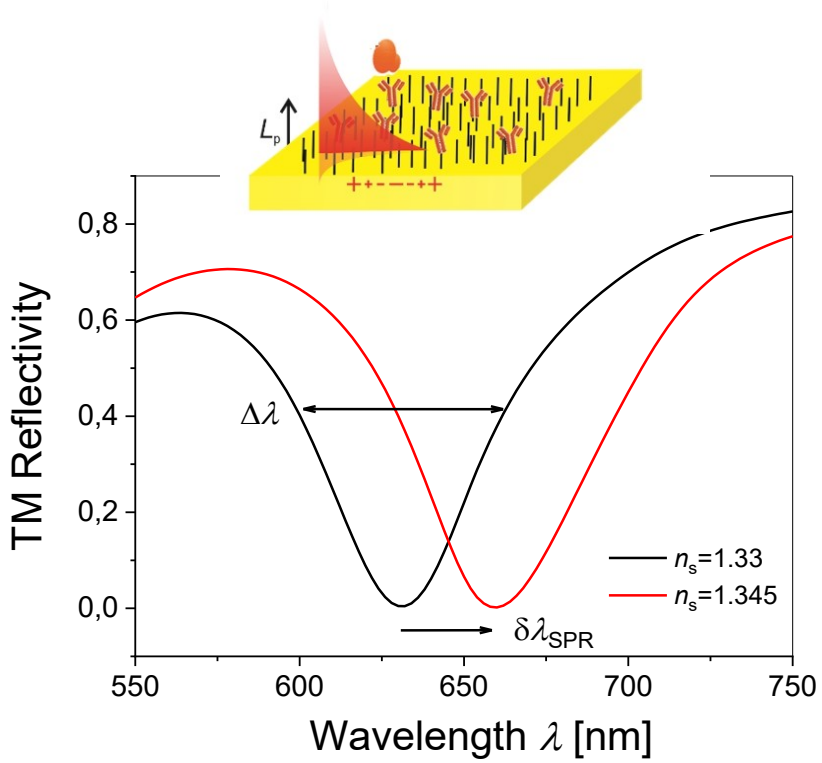

$S_b=\delta\lambda_{SPR}/\delta n_s$=2000 nm/RIU

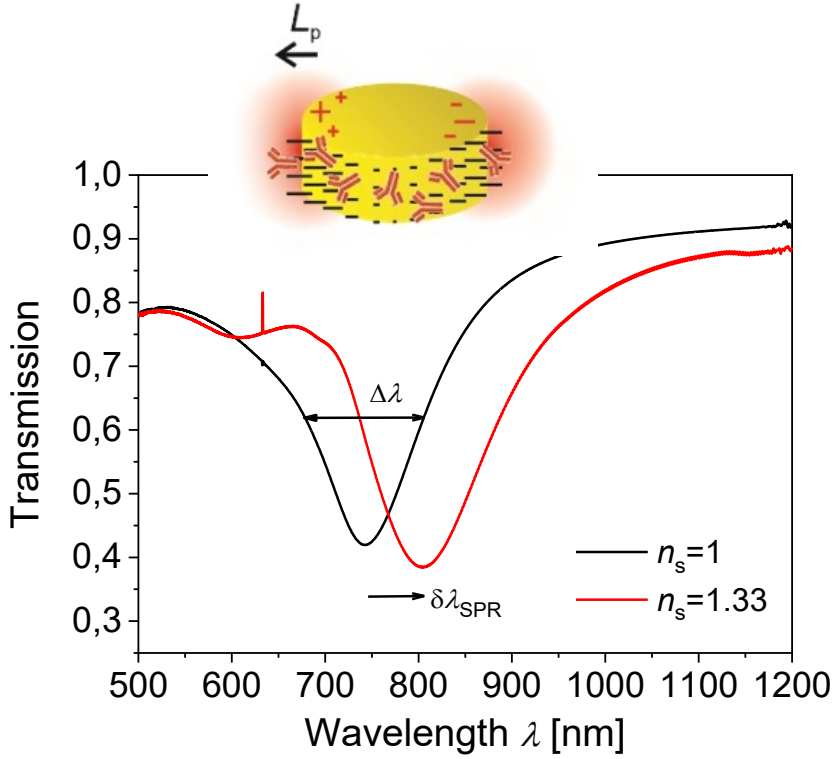

S_b=190 nm/RIU

A. Bozdogan, S. Hageneder, J. Dostalek, Plasmonic biosensors relying on biomolecular conformational changes: Case of odorant binding proteins, Methods in Enzymology, Elsevier (2020), ISSN 0076-6879.

Probing Depth – LSP and PSP

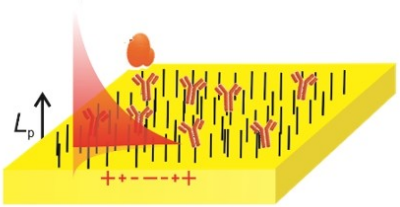

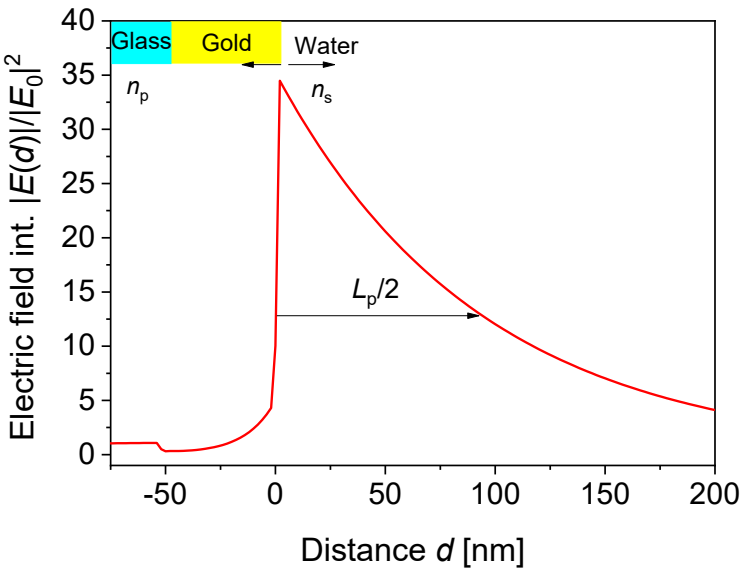

$L_p/2$=93 nm

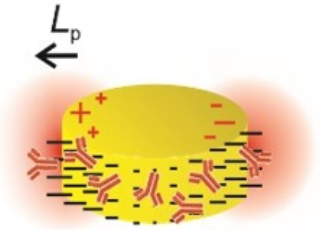

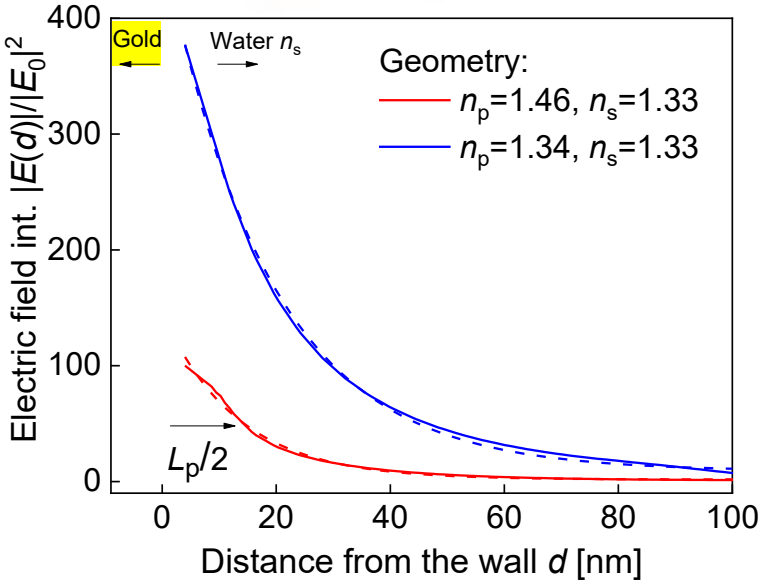

$L_p/2$=13-18 nm

A. Bozdogan, S. Hageneder, J. Dostalek, Plasmonic biosensors relying on biomolecular conformational changes: Case of odorant binding proteins, Methods in Enzymology, Elsevier (2020), ISSN 0076-6879.

SPR and LSPR Comparison

Both SPR and LSPR biosensors were applied for the analysis of chemical and biological analytes and range of instruments become commercially available

	SPR	LSPR
Complexity of instrument	high	simple
Refractive index resolution	10^{-7}	an order of mag. lower
Probing depth	> 100 nm	>10 nm
Parallelized detection	propagation length > 1 μm	individual NP possible

Kvasnicka et al, BIOINTERPHASES **Volume:** 3 **Issue:** 3 **Pages:** FD4-FD11 **DOI:** 10.1116/1.2994687. Stewart et al, Chem. Rev. 2008, 108, 494−521. Homola, **Chemical Reviews**, 108, 462-493 (2008).

Interrogation of SPR Changes

EUROPEAN UNION
European Structural and Investment Funds
Operational Programme Research, Development and Education
MINISTRY OF EDUCATION, YOUTH AND SPORTS
FZU Institute of Physics of the Czech Academy of Sciences
AIT AUSTRIAN INSTITUTE OF TECHNOLOGY

Intensity Modulation

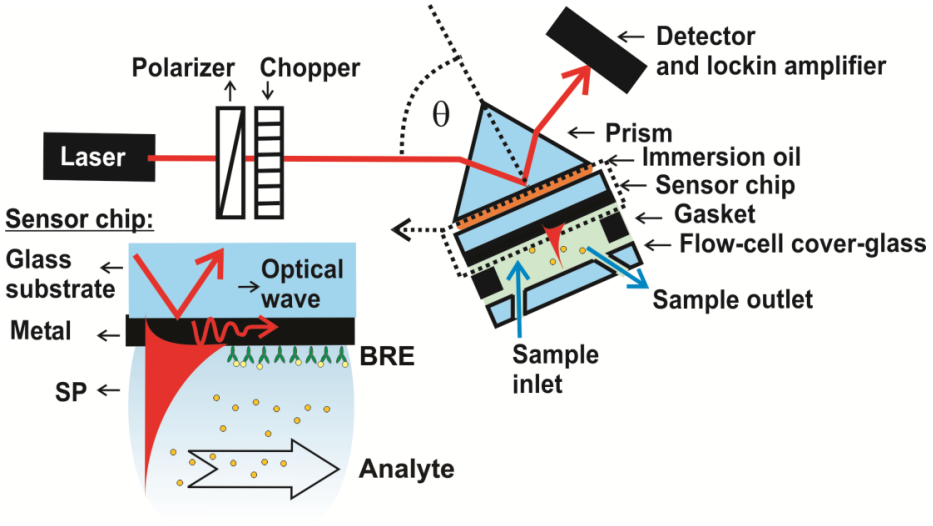

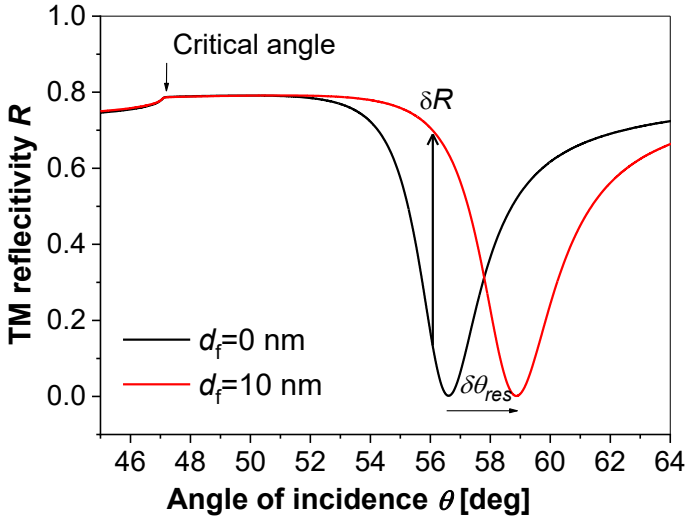

- Angle of incidence θ and wavelength λ are fixed at the edge of the SPR dip, where slope $\delta R/\delta\theta$ is highest.
- Simple implementation that allows for fast measurements of SPR changes
- Drawback is the small dynamic range, where δR shifts linearly with the measured changes (represented as a thickness of biolayer d_f).
- Typically the accuracy of the measurement is low (resolution 10^{-5} RIU).

Angular Modulation of SPR

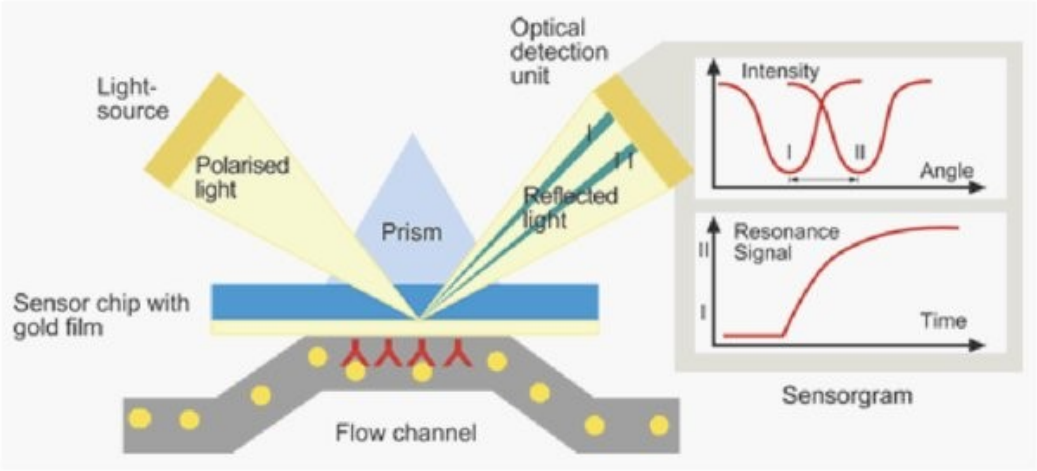

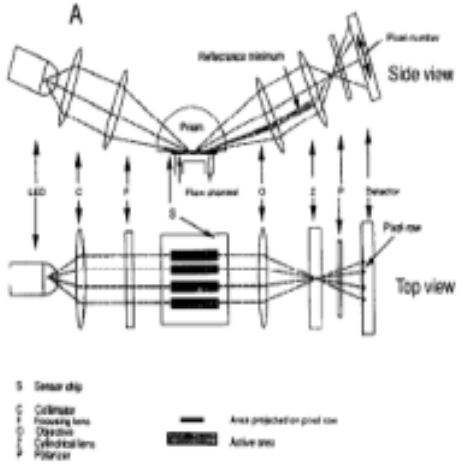

Liedberg, B., C. Nylander and I. Lundstrom Biosensing with surface plasmon resonance - how it all started. *Biosens.Bioelectron.* 10: i-ix; (1995)

- Measuring the whole reflectivity spectrum $R(\theta)$ by using a converging monochromatic optical beam (fixed λ) that is projected to a CCD detector (no movable parts). Introduced in early 1990ties by a Swedish company Farmacia Bioacore.
- Typically not versatile and build for specific refractive index range.
- Fast measurement of whole reflectivity spectrum allows for tracking of refractive index changes with high accuracy (resolution 10^{-7} RIU).

Wavelength Modulation of SPR

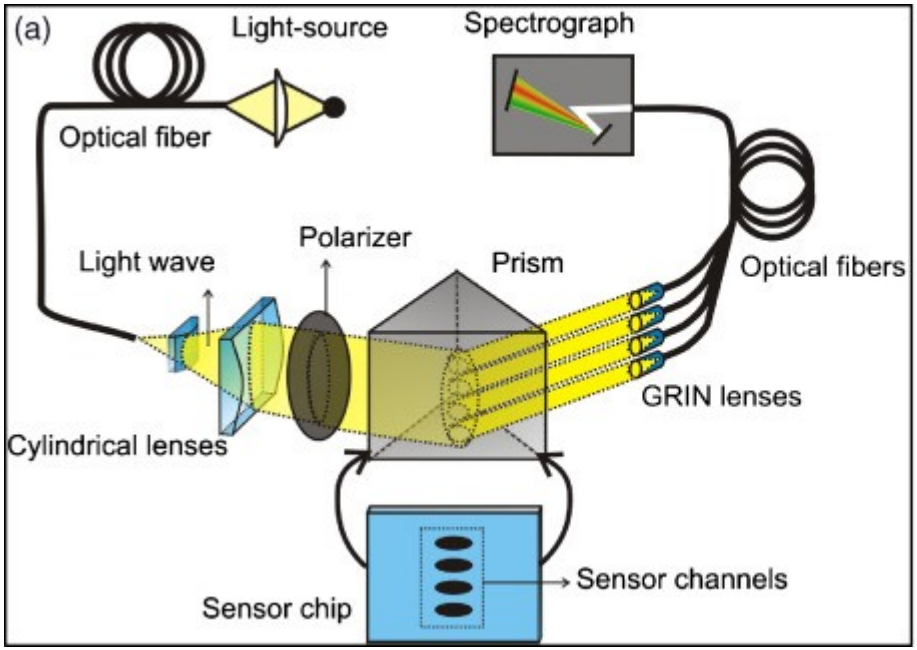

https://doi.org/10.1016/j.snb.2008.09.006

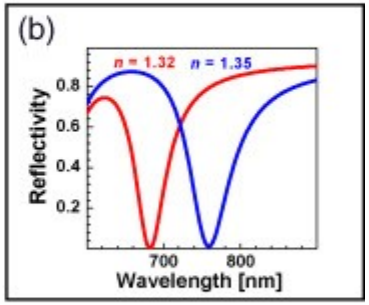

J. Homola, J. Dostalek, S. Chen, A. Rasooly, S. Jiang, S. S. Yee: Spectral Surface Plasmon Resonance Biosensor for Detection of Staphylococcal Enterotoxin B (SEB) in Milk , Journal of Microbiology, 75, (2002) 61-69.

- Measuring wavelength reflectivity spectrum $R(\lambda)$ for a fixed angle of incidence θ. The spectrum is analysed by a spectrometer that changes in resonant wavelength are tracked in time.
- No movable parts and high accuracy (10^{-7} RIU).
- The sensitivity is nonlinearly changing with wavelength λ.

Tracking of SPR Changes

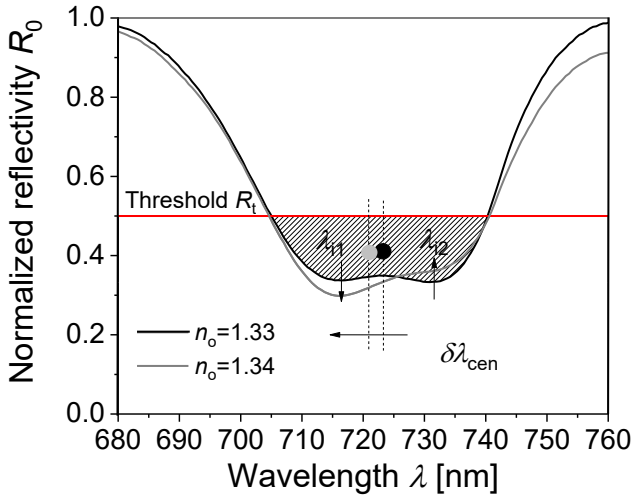

$$\lambda_{cen} = \sum_{i=N_1}^{N_2} \lambda_i \left[R_t - R_0(\lambda_i) \right] / \sum_{i=N_1}^{N_2} \left[R_t - R_0(\lambda_i) \right]$$

R_t – threshold
R_i – discrete reflectivity values
λ_i – discrete wavelength values

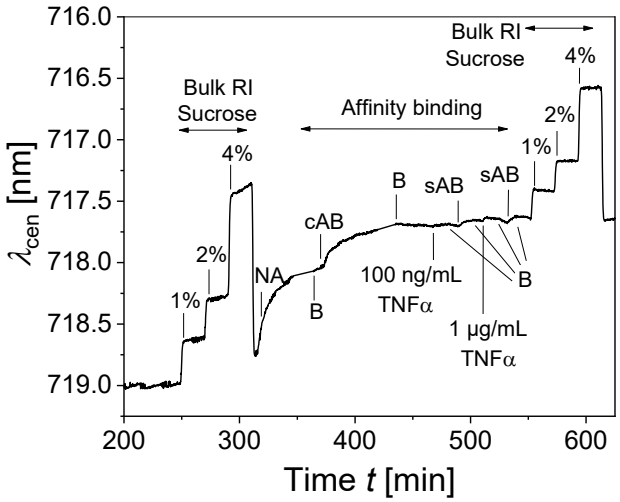

- Tracking of very small spectral shifts is possible ($\delta\lambda_{SPR}$<10^{-2} nm).
- Various approaches based on fitting of SPR reflectivity curves with analytical function or centroid method were used in SPR biosensors.

EUROPEAN UNION
European Structural and Investment Funds
Operational Programme Research,
Development and Education

MINISTRY OF EDUCATION, YOUTH AND SPORTS

FZU Institute of Physics of the Czech Academy of Sciences

AIT AUSTRIAN INSTITUTE OF TECHNOLOGY

Tracking of SPR Changes

Garet G Nenninger *et al* 2002 *Meas. Sci. Technol.* **13** 2038

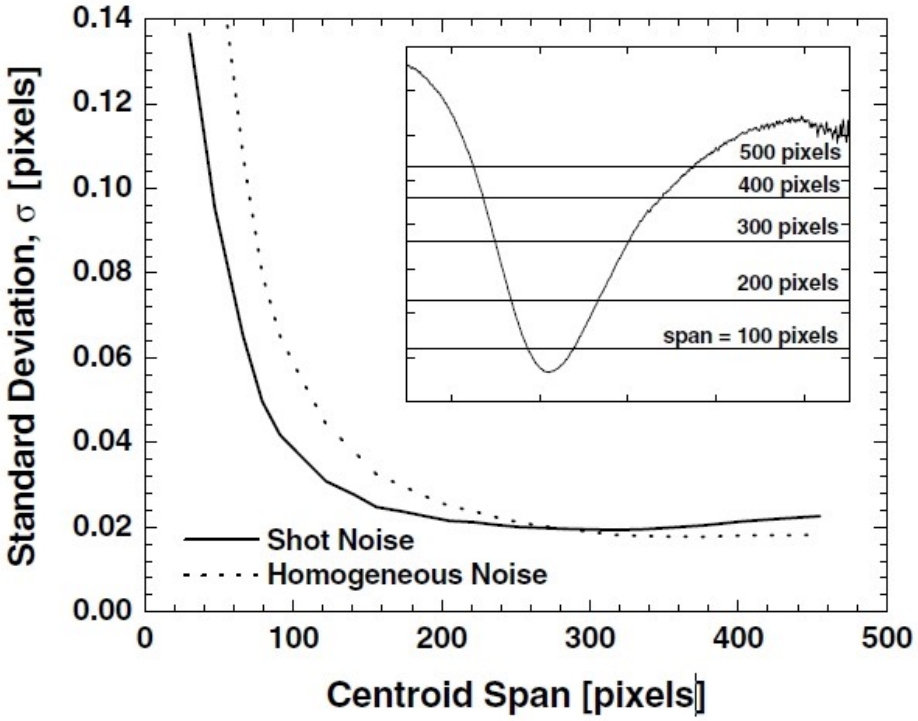

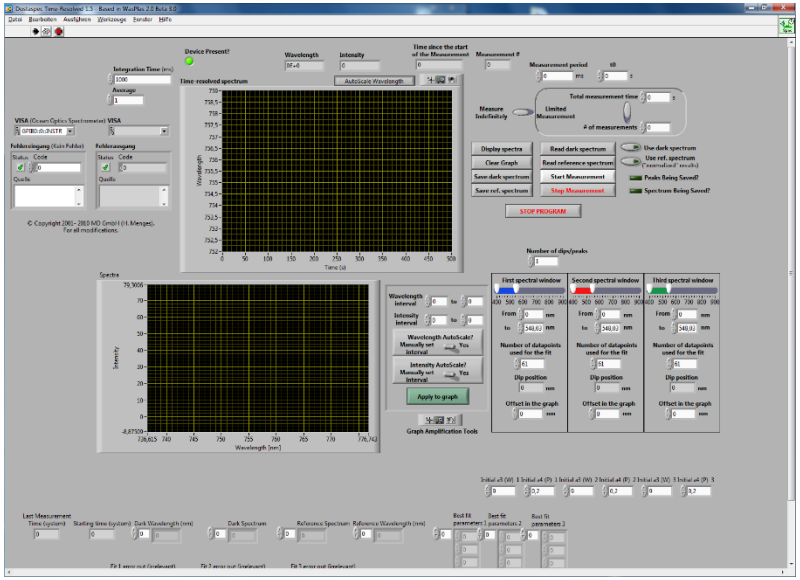

Nico's Labview software to track SPR wavelength changes by polynomial fitting or centroid.

- **Parameters of the tracking routine needs to be optimized in order to minimize the noise of the baseline signal λ_{cen}.**

EUROPEAN UNION
European Structural and Investment Funds
Operational Programme Research,
Development and Education

MINISTRY OF EDUCATION, YOUTH AND SPORTS

FZU Institute of Physics of the Czech Academy of Sciences

AIT AUSTRIAN INSTITUTE OF TECHNOLOGY

Key Characteristics

doi:10.1016/j.snb.2004.12.096

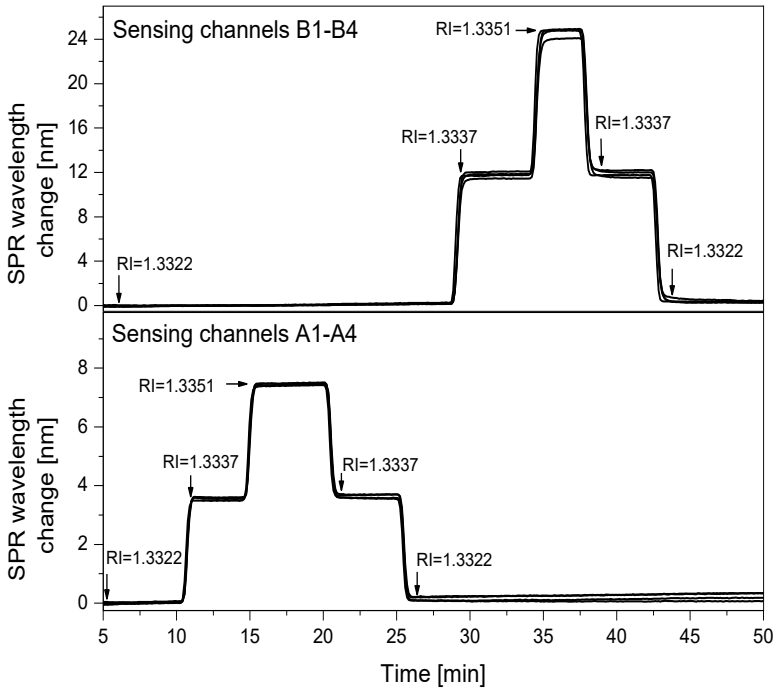

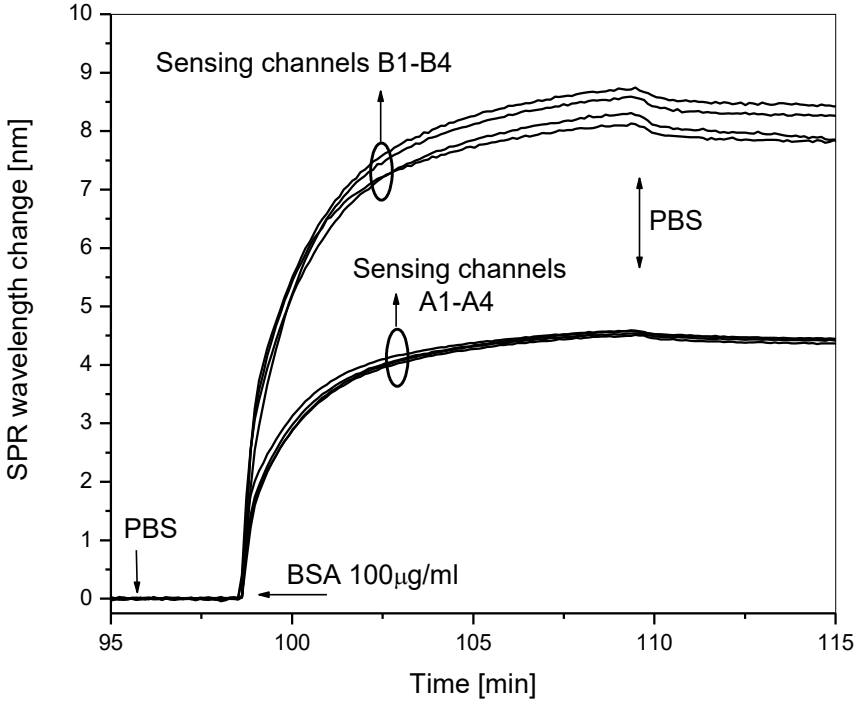

- Calibration with bulk refractive index change δn_b.
- Calibration with biolayer growth leading to surface mass density change $\Delta\Gamma$.

EUROPEAN UNION
European Structural and Investment Funds
Operational Programme Research, Development and Education

MINISTRY OF EDUCATION, YOUTH AND SPORTS

FZU Institute of Physics of the Czech Academy of Sciences

AIT AUSTRIAN INSTITUTE OF TECHNOLOGY

Key Characteristics

Bulk refractive index sensitivity $S_b = \delta\lambda_{res} / \delta n_d$

Sensor response in RIU $\delta\lambda_{res} / S_b$

Baseline noise $\sigma(\lambda_{res})$

Refractive index resolution $RI = \sigma(\lambda_{res}) / S_b$

Change due to molecular binding $\delta\lambda_{res} = S_s \Delta\Gamma$

Minimum detectable surface mass density change $\delta\Gamma = \sigma(\lambda_{res}) / S_s$

Minimum detectable surface density $\delta\Gamma / MW$

- **Refractive index resolution (10^{-7}) and minimum detectable surface mass density change (pg/mm^2) can be used as universal characteristics of SPR biosensor instruments.**

Surface Mass Density Measurements

EUROPEAN UNION
European Structural and Investment Funds
Operational Programme Research, Development and Education
MINISTRY OF EDUCATION, YOUTH AND SPORTS
FZU Institute of Physics of the Czech Academy of Sciences
AIT AUSTRIAN INSTITUTE OF TECHNOLOGY

Observation of Thin Biomolecular Films

- SPR response ($\delta\theta_{res}$) proportional to mass adhered to the surface Γ.

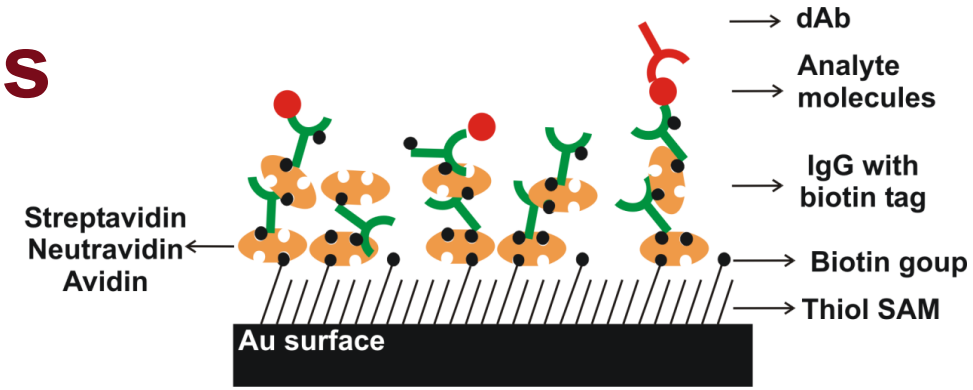

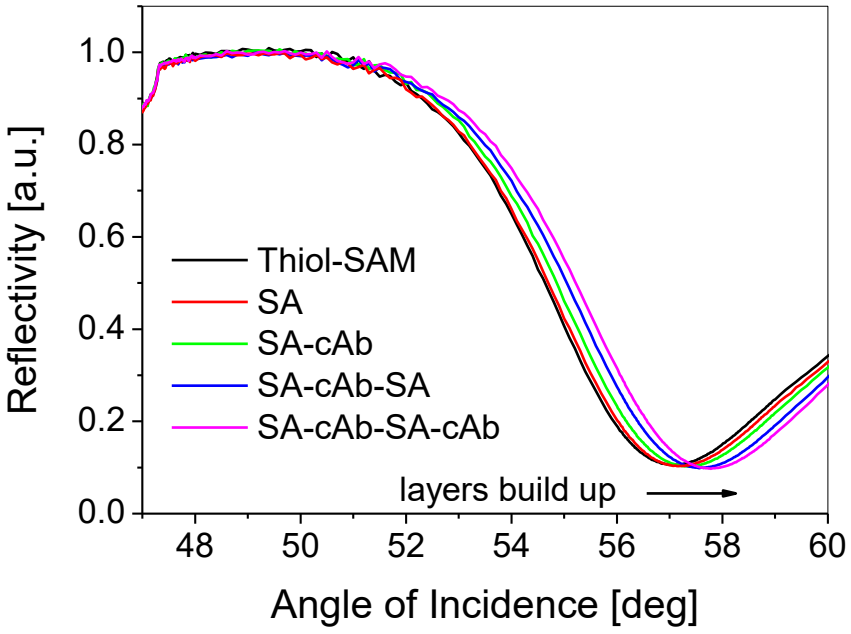

Layer-by-layer building up of SA/cAb.

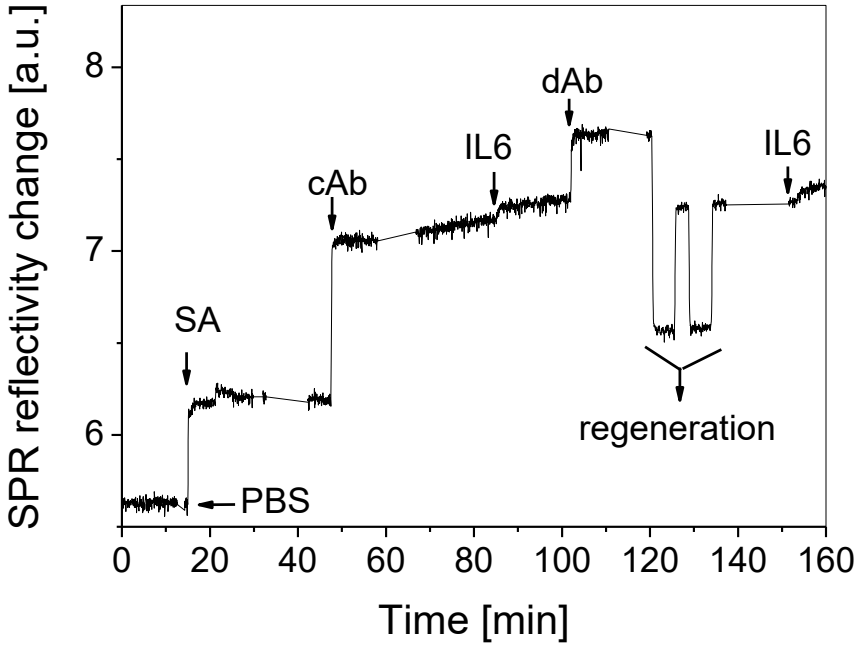

SPR IL6 sandwich assay.

Observation of Thin Biomolecular Films

SPR signal change can be converted to the surface mass density of bound biomolecules Γ. Useful tool for the investigation of surface coverage of proteins, binding capacity, developing assays….

Fitting of SPR spectra allows determining of refractive index n_f and / or thickness d_f of thin films (*e.g.,* implemented in a software Winspall).

$$\Gamma = (n_f - n_d) d_f \frac{\partial c}{\partial n_f}$$

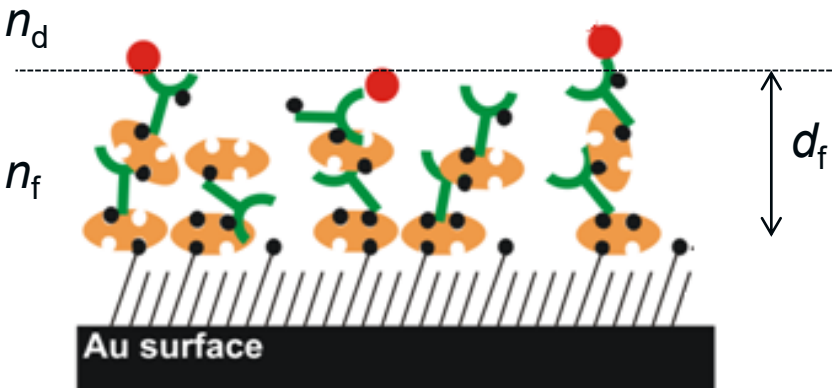

For most polymer materials holds $\partial n_f / \partial c \sim 0.2$ mm^3 mg^{-1} and in aqueous samples n_d=1.33. For instance a full packed IgG monolayer exhibits $\Gamma \sim 4$ ng/mm^2, IgG hydrodynamic radius $R_h \sim 5$ nm.

EUROPEAN UNION
European Structural and Investment Funds
Operational Programme Research,
Development and Education

MINISTRY OF EDUCATION,
YOUTH AND SPORTS

FZU Institute of Physics of the Czech Academy of Sciences

AIT AUSTRIAN INSTITUTE OF TECHNOLOGY

‘Mainz’ SPR Biosensors

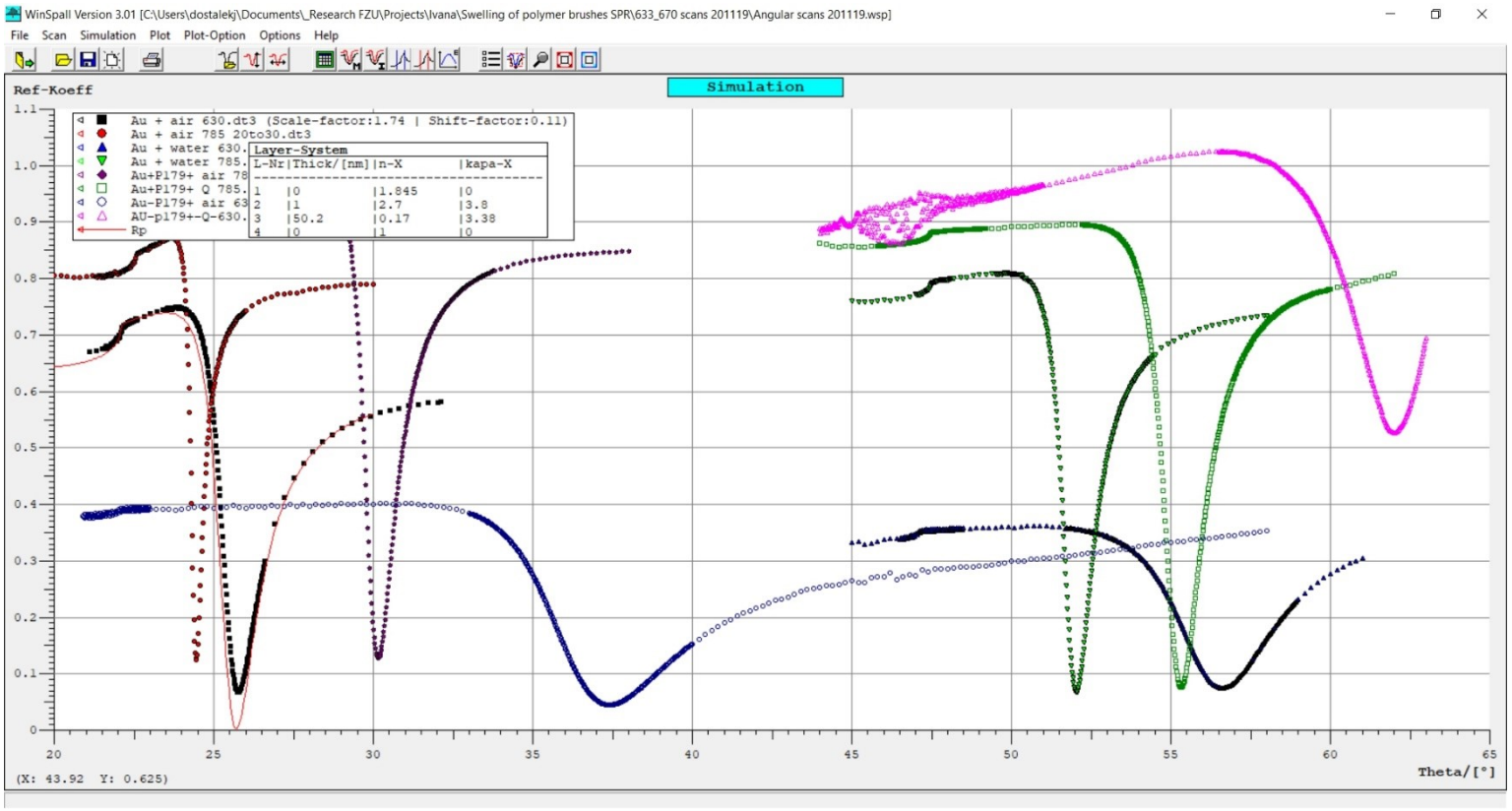

- Fitting of reflectivity curves allows to determine the thickness d_f and refractive index n_f in order to determine the surface mass density Γ.